The Traffic Reaction Model: A kinetic compartmental approach to road traffic modeling

(article starts on next page)

The Traffic Reaction Model: A kinetic compartmental approach to road traffic modeling[☆]

M. Pereira [a,d,*], B. Kulcsár [a], Gy. Lipták [b,c], M. Kovács [c], G. Szederkényi [b,c]

[a] *Department of Electrical Engineering, Chalmers University of Technology, Gothenburg, Sweden*
[b] *Institute for Computer Science and Control (SZTAKI), Budapest, Hungary*
[c] *Faculty of Information Technology and Bionics, Pázmány Péter Catholic University, Budapest, Hungary*
[d] *Center for Geosciences and Geoengineering, Mines Paris - PSL University, Fontainebleau, France*

ARTICLE INFO

ABSTRACT

In this work, a family of finite volume discretization schemes for LWR-type first order traffic flow models (with possible on- and off-ramps) is proposed: the Traffic Reaction Model (TRM). These schemes yield systems of ODEs that are formally equivalent to the kinetic systems used to model chemical reaction networks. An in-depth numerical analysis of the TRM is performed. On the one hand, the analytical properties of the scheme (nonnegative, conservative, capacity-preserving, monotone) and its relation to more traditional schemes for traffic flow models (Godunov, CTM) are presented. Finally, the link between the TRM and kinetic systems is exploited to offer a novel compartmental interpretation of traffic models. In particular, kinetic theory is used to derive dynamical properties (namely persistence and Lyapunov stability) of the TRM for a specific road configuration. Two extensions of the proposed model, to networks and changing driving conditions, are also described.

1. Introduction

Macroscopic traffic flow models play an important role in the analysis, simulation, and control of traffic flows on networks (Siri et al., 2021; Piccoli and Rascle, 2013; Treiber et al., 2013; Papageorgiou, 1983; Karafyllis et al., 2018; Karafyllis and Papageorgiou, 2019; Coogan and Arcak, 2016; Jin, 2021). In this line of research, first order traffic flow models, that describe the spatio-temporal evolution of the vehicular density through conservation laws, predominate in the literature (Garavello et al., 2016; Tordeux et al., 2018). These models, e.g. Garavello et al. (2016), Haight (1963), Lighthill and Whitham (1955) and Daganzo (1994), express the conservation of vehicles on the road by linking the density and the flux of vehicles in space and time. In particular, Lighthill and Whitham (1955), and Richards (1956) suggested to further assume that the flux of vehicles can be expressed as function of the density called flux function (or fundamental diagram). The resulting traffic model, called Lighthill–Whitham–Richards (LWR) model, has been extensively studied and takes the form of a nonlinear hyperbolic Partial Differential Equation (hPDE) satisfied by the density of vehicles (Bressan, 2000; Treiber et al., 2013). In general, no closed-form solution is available to solve such hPDEs and therefore *appropriate* numerical approximations must be introduced.

Finite Volume Methods (FVMs) have been particularly praised for deriving numerical solutions of conservation laws, especially for their ability to accurately describe the singularities specific to these hPDEs (e.g. shock waves) (Leveque, 1992; Bressan, 2000). The Godunov scheme (Godunov, 1959) is an instance of such methods widely used in traffic flow modeling for its advantageous theoretical and convergence properties (Leveque, 1992). For instance, Daganzo proposes to equip the traditional Godunov scheme (Godunov, 1959) with static saturation functions (capacitated sending-receiving flows between cells), thus yielding the so-called Cell Transmission Model (CTM) (Daganzo, 1994). This model is convenient in terms of describing capacity changes and has been the basis of many traffic network control solutions e.g. Csikos and Kulcsar (2017).

The choice of numerical scheme is instrumental in deriving proper approximations of the solution of the considered hPDEs. First, the numerical approximations at hand need to preserve several important properties of the original hPDE like the nonnegativity of the solution or the fact that it should be bounded by the road capacity at all times. Besides, when it comes to FVMs, their stability (Eymard et al., 2000) can be assessed by analyzing the systems of ordinary differential equations (ODEs) resulting from the space discretization of the PDE. These systems of ODEs may then have a connection to an already existing modeling framework thus facilitating their analysis.

On the other hand, positive (or nonnegative) systems having the property that the state variables are always nonnegative have a distinguished role in systems and control theory due to the wide field of possible applications e.g., in thermodynamics, chemistry, biology or economy (Farina and Rinaldi, 2000). Moreover, the positivity of the states efficiently supports dynamical analysis and control design (Haddad et al., 2010). Within nonnegative systems, kinetic models (also called chemical reaction networks or CRNs) and the closely related compartmental models are good descriptors of complex nonlinear dynamics, and their mathematical and corresponding graph structure are intuitive and useful to state strong results on qualitative dynamics (Érdi and Tóth, 1989; Jacquez and Simon, 1993). The theory of kinetic systems is a rapidly developing area of increasing interest where the most significant contributions are related to the existence and uniqueness of equilibria and robust stability even when several model parameters (possibly including time delays) are not precisely known or unknown (Feinberg, 2019). Therefore, it is of general interest to transform originally non-chemical models to kinetic form, and interpret or discover their properties from this point of view (Samardzija et al., 1989).

Building on these ideas, we propose and study a family of finite volume approximations of the LWR model, called Traffic Reaction Model (TRM), with direct links to the positive kinetic systems used to model chemical reaction networks (Feinberg, 2019; Szederkényi et al., 2018). The benefits of this analogy are multiple. On the one hand, the resulting model provides a new interpretation of the discrete dynamics of the LWR model as a compartmental chemical system in which the concentration of "particles" of free and occupied space are exchanged between adjacent road cells. This analogy also allows to straightforwardly extend the LWR model to better represent traffic conditions that can occur in real life (e.g. merging, changing road conditions, traffic lights).

Invariance and symmetry properties have extensively been researched in kinematic wave theory e.g. Newell (1993a,b,c), Daganzo (2005) and Laval and Leclercq (2013). In the latter two papers, duality plays a key role to bridge the gap between coordinates in which traffic flow models are presented. A key consequence is that variational theory enables us to connect homogeneous first order traffic flow models with proper initial and boundary value problems. In Laval and Chilukuri (2016), the authors explore the symmetry of kinematic wave models under coordinates transformation and dual variable changes. When dualized, it is shown that travel time, delay, and flow remain invariant. In our paper, flow invariance is in the epicenter of TRM (through the re-definition of the flux by the dual state variable). The dual state variable is the free space concentration or dual density, which ensures the invariance of the nonlinear flux function via a non-unique parametrization and decomposition. However, unlike in Laval and Chilukuri (2016), we do not try to explicitly transform the conservation laws and define new coordinates to ease delay or capacity calculations (for triangular fundamental diagrams). Instead, we use a nonlinear flux function, and decompose and parameterize it with the dual state variable (free space), where no coordinates transformation is required. Via the dual state variable and with the help of the flux decomposition, the numerical segmentation of the hyperbolic PDE (TRM) preserves several fundamental properties (e.g. non-negativity, capacity, etc.). Furthermore, TRM can handle (under some mild conditions) inhomogeneity in PDEs and can accommodate a wide set of nonlinear flux functions. Finally, the system of nonlinear ODEs obtained by the TRM scheme can be interpreted as particular instances of kinetic dynamical systems which can be formally represented as chemical reactions. This special description opens the way to leverage the extensive literature on reaction networks to derive and analyze the dynamical properties of the system (such as robustness or stability) (Feinberg, 1987; Chaves and Sontag, 2002; Sontag, 2001; Shinar and Feinberg, 2010), and even propose novel optimal control strategies and traffic management techniques (Shinar and Feinberg, 2010; Coogan and Arcak, 2015) towards (Csikós et al., 2017; Dabiri and Kulcsár, 2015; Dabiri et al., 2017).

The main contributions of this work are as follows. Firstly, we propose an in-depth analysis of the TRM as a numerical scheme. We prove that it defines is consistent, monotone, nonnegative, capacity-preserving, and conservative numerical schemes. We also draw parallels between the TRM and existing methods, showing in particular that the TRM is in fact equivalent to a generic formulation of Daganzo's CTM, and that the Godunov scheme can be seen as particular instance of TRM. Consequently, both methods can also be treated as particular kinetic systems and the results from kinetic system theory can also be extended to them.

Secondly, we provide the arguments allowing to bridge the gap between numerical schemes for traffic models and kinetic systems for chemical reaction networks. We provide detailed physical interpretations of how traffic flow is apprehended when seen as a kinetic system. We then leverage the link between the TRM and kinetic systems to provide an analysis of some dynamical properties of the TRM in a particular case. Persistence is introduced as new concept for traffic flow models based on this parallel. Also the structure and stability of the equilibria of the system are studied using Lyapunov theory for kinetic systems.

Finally, we present two direct extensions of the TRM that directly follow from the kinetic interpretation of traffic proposed in this work. The first one accounts for changing road conditions. Such extensions can be used to accurately model real traffic data set in state estimation and short-term prediction applications, as advocated in Pereira et al. (2022a,b). The second extension allows us to describe traffic on road networks. In this aspect, the TRM hints to model the link and node behavior identically using reaction rate governed mixing compartments, giving rise to a smooth interface between link and node modeling framework. Furthermore, the network extension of TRM fits in the genealogy of first order node models presented in Tampère et al. (2011). The network extended TRM fulfills the requirements for node models described in Tampère et al. (2011), where most of the properties are preserved thanks to the applied non-negative discretization scheme. Interestingly, many of the requirements are of continuous nature (e.g. conservation, capacity, non-negativity, or invariance) and no external constraints need to be enforced to guarantee them. It is important to note that the *Network TRM* presented in this paper covers only non-signalized intersections.

The outline of the paper is as follows. In Section 2, we introduce the TRM as a finite volume scheme for the LWR model and describe its main properties. We then expose in Section 3 the coupling that exists between kinetic reaction theory and the TRM. In Section 4, we provide an analysis of the TRM through its interpretation as particular case of CTM and a numerical experiment testing the convergence and accuracy of the TRM. In Section 3.3, we derive some dynamical properties (namely persistence and Lyapunov stability) of the TRM when considered on a circular road. Finally, we present in Section 5 the two extensions of the TRM discussed above.

2. Nonnegative discretization of hyperbolic PDEs

The Lighthill–Whitham–Richards (LWR) traffic model (Lighthill and Whitham, 1955) is the first-order macroscopic traffic flow model defined by the following partial differential equation (PDE) on the domain $\mathbb{R} \times \overline{\mathbb{R}}_+$

$$\partial_t \rho + \partial_x f(\rho)_x = r - s, \tag{1}$$

This PDE models the space–time evolution of a conserved quantity $\rho(x,t) \in \Omega = [0, \rho_{\max}]$ corresponding to to the traffic density on a road, where $\rho_{\max}$ denotes the maximal vehicle density. The flux of vehicles is represented $f \circ \rho$, for some continuous and at least once differentiable $f : \mathbb{R} \to \mathbb{R}$ called flux function. In particular, we denote by ρ_{crit} the critical density value at which the flux attains its maximal value $f_{\max}$ (i.e. $f_{\max} = f(\rho_{\mathrm{crit}})$). Finally, the functions r, s model the on- and off-ramps, respectively.

Remark 2.1. We consider physically-relevant (weak) solutions ρ of PDE (1) also called entropy solutions. We refer the reader to Appendix A for a result justifying the existence and uniqueness of an entropy solution, and the regularity of this solution under non-zero sink and source terms.

To mirror the vehicle density ρ, we introduce a function v modeling the density of free space (i.e. unoccupied by a vehicle) along the road, and given by

$$v = \rho_{\max} - \rho.$$

We set $v_{\max} = \rho_{\max}$. Note then that the free space density v can be seen as a dual or adjoint variable to the density ρ.[1] In this work, we consider the case where the flux function f has the form

$$f(\rho) = g(\rho, v) = g(\rho, \rho_{\max} - \rho), \tag{2}$$

where $g : \Omega \times \Omega \mapsto \overline{\mathbb{R}}_+$ satisfies the following assumptions[2]:

(A1) g is Lipschitz continuous w.r.t. both arguments, with associated Lipschitz constants $K_1 > 0$ and $K_2 > 0$,

(A2) g is non-decreasing in each arguments,

(A3) $g(\rho, 0) = g(0, v) = 0$ for all $\rho, v \in \Omega$ which ensures that no vehicles is removed (resp. added) if the road is empty (resp. at capacity).

Example 1. Any flux function f that can be written as

$$f(\rho) = g_1(\rho)g_2(\rho_{\max} - \rho), \quad \rho \in \Omega,$$

where g_1 and g_2 are non-decreasing Lipschitz-continuous functions such that $g_1(0) = g_2(0) = 0$ satisfy Assumptions (A1)–(A3). In particular, if we take $g_1(\rho) = \rho$, then the function $\rho \mapsto g_2(\rho_{\max} - \rho)$ can be interpreted as the speed-density relationship of the fundamental diagram. Within this framework, taking $g_2(v) \propto v$ yields the Greenshields (quadratic) flux function (cf. Fig. 1). We can also retrieve trapezoidal fundamental diagrams by considering g_2 as

$$g_2(v) = \begin{cases} v_{\max} \frac{\rho_{\max} - v_1}{\rho_{\max} - v} \frac{v}{v_2} & \text{if } 0 \leq v \leq v_2, \\ v_{\max} \frac{\rho_{\max} - v_1}{\rho_{\max} - v} & \text{if } v_2 \leq v \leq v_1, \\ v_{\max} & \text{if } v_1 \leq v \leq v_{\max}, \end{cases}$$

---

[1] v is the concentration or density of free spaces.

[2] These requirements are inspired by the properties of chemical reaction rates, as it will be explained in Section 3.

(a) Flux-density relationship

(b) Speed-density relationship (Function $\rho \mapsto g_2(\rho_{\max} - \rho)$)
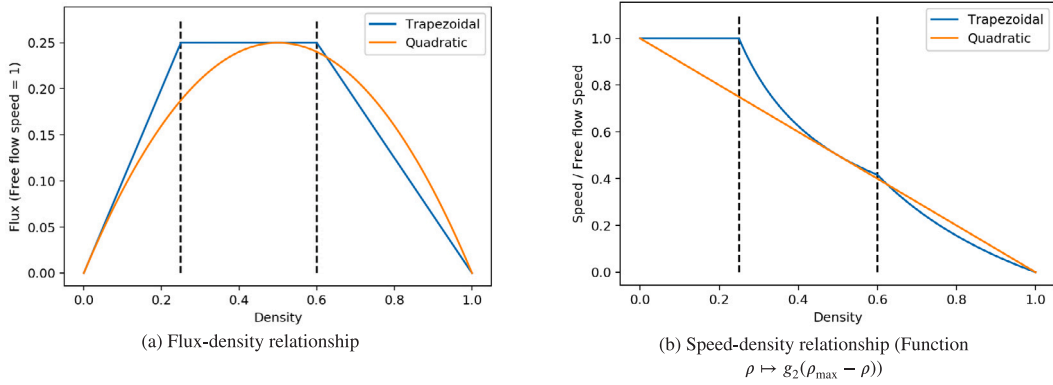
Fig. 1. Comparison between quadratic and trapezoidal fundamental diagrams. The maximal density $\rho_{\max}$ and the free flow speed $v_{\max}$ are taken equal to 1. The black dotted lines are placed at the critical density values $\rho_1 = 0.25$ and $\rho_2 = 0.6$.

where $v_{\max}$ denotes the free flow speed, and $\rho_1 = \rho_{\max} - v_1$, $\rho_2 = \rho_{\max} - v_2$ denote the critical densities of the fundamental diagram which satisfy $0 < \rho_1 \leq \rho_2 < \rho_{\max}$. Fig. 1 gives an example of a trapezoidal flux function obtained using this decomposition.

Regarding the source and sink terms, we assume that they can be written for any $(x, \rho, t) \in \mathbb{R} \times \Omega \times \mathbb{R}_+$ as:

$$r(x, t, \rho) = 1_{\text{on}}(x) g_{\text{on}}(\rho_{\text{on}}(x, t), v), \quad s(x, t, \rho) = 1_{\text{off}}(x) g_{\text{off}}(\rho, v_{\text{off}}(x, t)), \tag{3}$$

where

- the functions ρ_{on} and v_{off} are the traffic density of the on-ramp and the free space density of the off-ramp, respectively, and are assumed to be taking values in Ω;
- the functions $g_{\text{on}} : \Omega \times \Omega \mapsto \overline{\mathbb{R}}_+$ and $g_{\text{off}} : \Omega \times \Omega \mapsto \overline{\mathbb{R}}_+$ are the traffic flows of the on- and off-ramp, respectively, and are assumed to satisfy Assumptions (A1)–(A3);
- the spatial position of the on- and off-ramp is described by indicator functions 1_{on} and 1_{off} defined as

$$1_{\text{on}}(x) = \begin{cases} 1, & \text{if } \underline{x}_{\text{on}} \leq x \leq \overline{x}_{\text{on}} \\ 0, & \text{otherwise} \end{cases}, \quad 1_{\text{off}}(x) = \begin{cases} 1, & \text{if } \underline{x}_{\text{off}} \leq x \leq \overline{x}_{\text{off}} \\ 0, & \text{otherwise} \end{cases},$$

for some $\underline{x}_{\text{on}} \leq \overline{x}_{\text{on}}$ and $\underline{x}_{\text{off}} \leq \overline{x}_{\text{off}}$.

We use the Finite Volume Method (FVM) to spatially discretize (i.e. semi-discretize) the conservation law model (1) with flux (2), source and sink (3) functions. To do so, we start by slicing the road into cells of length $\Delta x > 0$, and centered at the points $x_i = i\Delta x$, for $i \in \mathbb{Z}$. We denote by I the set of road cell indices (hence $I = \mathbb{Z}$ for an infinite road) and denote by $x_{i-1/2}$ and $x_{i+1/2}$ the left and right boundary of the ith cell, respectively, and by $C_i = [x_{i-1/2}, x_{i+1/2}]$ the ith cell. Then, the FVM scheme can be written as

$$\dot{\rho}_i(t) = \frac{1}{\Delta x} \left(F(\rho_{i-1}, \rho_i) - F(\rho_i, \rho_{i+1}) + R_i(\rho_i, t) - S_i(\rho_i, t) \right), \quad i \in I, \quad t \geq 0, \tag{4}$$

where ρ_i is an approximation of the average traffic density over the ith cell, the so-called numerical flux F is given by $F(u, v) = g(u, \rho_{\max} - v)$, and the numerical source R_i and sink S_i terms are given (for $t \geq 0, i \in I$) by

$$R_i(\rho, t) = \int_{C_i} r(x, \rho, t) dx, \quad S_i(\rho, t) = \int_{C_i} s(x, \rho, t) dx.$$

We call *Traffic Reaction Model* (TRM) the resulting model which describes traffic along a (discretized) road. Note that this model is control-oriented since changing g and/or $g_{\text{on}}, g_{\text{off}}$ corresponds to speed limit control and/or ramp metering. We also take as initial condition:

$$\rho_i(0) = \frac{1}{\Delta x} \int_{C_i} \rho(x, 0) \, dx \in \Omega, \quad i \in I.$$

As such, the TRM defines a particular instance of finite volume scheme for scalar conservation laws (LeVeque et al., 2002; Chainais-Hillairet and Champier, 2001).

Finally, note that in practice, finite roads should be considered. To be able to use the TRM to model traffic on a finite road, boundary conditions describing the incoming and outgoing traffic on the road have to be defined. Assuming that the road is now discretized into P cells with indices $i \in I = \{1, \dots, P\}$, the density of vehicles on these cells is modeled using the system of ODEs defined by (4) while assuming that the quantities ρ_0 and ρ_{P+1} are some specific time-dependent functions taking values in Ω. For instance, these functions can be set so that the quantities $F(\rho_0, \rho_1)$ and $F(\rho_P, \rho_{P+1})$ match some known incoming and outgoing fluxes

in the road. Another possibility is to set $\rho_0 = \rho_P$ and $\rho_{P+1} = \rho_1$, which corresponds to periodic boundary conditions, or equivalently a circular road.

We now present a few numerical properties of the TRM, which hold whether the road is finite or not (cf. Appendix B.1 for proof).

Theorem 2.2. *The numerical flux F is consistent with the flux function f (i.e. it satisfies for any $u \in \Omega$, $F(u, u) = f(u)$) and is monotone. As for the TRM defined in* (4)*, it preserves nonnegativity and capacity, and it is conservative finite volume scheme.*

It is important to note that, for a given f the choice of g is not unique. Hence, the TRM defines a family of numerical discretization schemes by means of the decomposition of the flux $f(\rho)$ in (2), which all share the properties described in Theorem 2.2.

Example 2. Consider the so-called Greenshield flux function defined by

$$f(\rho) = \rho \, v(\rho), \text{ with } v(\rho) = \omega(\rho_{\max} - \rho), \quad \rho \in \Omega,$$

where v is the average vehicle speed, and $\omega = v_{\max} / \rho_{\max}$ with the free flow speed $v_{\max} > 0$. Different decompositions of f as in (2) can be proposed, among which:

$$g_{\text{MAK}}(\rho, v) = \omega \rho v, \tag{5}$$

$$g_{\text{Gdnv}}(\rho, v) = \min(D(\rho), Q(\rho_{\max} - v)), \tag{6}$$

$$g_{\text{Cap}}(\rho, v) = D(\rho)Q(\rho_{\max} - v)/f_{\max},$$

where $D(\rho) = f(\min\{\rho, \rho_{\text{crit}}\})$, $Q(\rho) = f(\max(\rho, \rho_{\text{crit}}))$ are the supply and demand functions, respectively, and $f_{\max}$ denotes the maximal value of the flux. Note in particular that the decomposition $g_{\text{Gdnv}}(\rho, v)$ in (6) is the Godunov flux, meaning that the Godunov scheme can be seen as a particular instance of TRM.

In the remainder of this text, we refer to the decomposition g_{MAK} in (5) as a mass action kinetic (MAK) decomposition.

We further discretize the TRM by considering a time step $\Delta t > 0$ and taking $t_k = k\Delta t$, $k \in \mathbb{N}_0$. We then define the fully-discrete TRM to be sequence of values $\{\rho_i^k : i \in I, k \in \mathbb{N}_0\}$ defined by the recurrence relations:

$$\rho_i^{k+1} = \rho_i^k + \frac{\Delta t}{\Delta x}\left(F(\rho_{i-1}^k, \rho_i^k) - F(\rho_i^k, \rho_{i+1}^k) + q_i^k\right), \tag{7}$$

$$\rho_i^0 = \rho_i(0) \in \Omega,$$

where the term q_i^k is given by

$$q_i^k = \frac{1}{\Delta t}\left[\int_{t_k}^{t_{k+1}} R_i(\rho_i^k, t)dt - \int_{t_k}^{t_{k+1}} S_i(\rho_i^k, t)dt\right].$$

In particular, if the road is finite, the quantities ρ_j^k, $j \in \{0, P+1\}$ are defined from the functions ρ_j as $\rho_j^k = (1/\Delta t)\int_{t_k}^{t_{k+1}} \rho_j(t)dt$. The next result exposes the conditions under which fully-discrete TRM converges to the solution of the PDE. It relies on the following assumption on the source r and sink s terms.

Assumption 2.3. The source and sink term $q = r - s$ of PDE (1) is bounded and such that for any $\rho \in \mathbb{R}$, $(x, t) \mapsto q(x, t, \rho)$ is Lipschitz-continuous (with a constant independent of u) and for any $(x, t) \in \mathbb{R} \times \mathbb{R}_+$, $\rho \mapsto q(x, t, \rho)$ is locally Lipschitz-continuous (with a constant independent of (x, t) and bounded K_1 and K_2 as defined in (A1)).

Theorem 2.4. *Let us assume that the source and sink term $q = r - s$ of PDE (1) satisfy Assumption 2.3 and that the following Courant-Friedrichs-Levy (CFL) condition is fulfilled:*

$$\frac{\Delta t}{\Delta x} \leq \frac{1}{K_1 + K_2}, \tag{8}$$

where K_1 and K_2 are defined in (A1)*. Then, the fully discrete TRM converges (in $L^1_{loc}(\mathbb{R} \times \mathbb{R}_+)$) towards the entropy solution of PDE (1) as $\Delta x, \Delta t \to 0$, with $\Delta t / \Delta x$ kept fixed and satisfying the CFL condition.*

Proof. This result is a direct application of Theorem 1 of Chainais-Hillairet and Champier (2001), which holds since the discretized scheme is monotone (cf. Theorem 2.2) and following from the assumptions on the regularity of the source and sink term q. $\square$

Remark 2.5. In the absence of source and sink terms (and with an infinite road), but under the CFL condition (8), the discretized numerical scheme in (7) is L^∞-stable, meaning that for any $(i, k) \in \mathbb{Z} \times \mathbb{N}_0$, $\rho_i^k \in [\min_{j \in \mathbb{Z}} \rho_j^0, \max_{j \in \mathbb{Z}} \rho_j^0]$ (cf. Lemma 21.1 in Eymard et al. (2000)). Consequently, the discrete numerical scheme preserves nonnegativity and capacity (as long as the initial condition is in Ω). Furthermore, since the scheme is monotone and L^∞-stable, it is Total Variation Diminishing (TVD) (Leveque, 1992, Theorems 15.4 & 15.5). As a consequence, the TRM is in particular shock-capturing. It implicitly incorporates correct jump conditions (without oscillations) near discontinuities when Δx and Δt tend to 0. Besides, the convergence of the (fully-discrete) TRM towards the PDE solution is of order at most 1 (LeVeque et al., 2002). We retrieved this behavior in numerical experiments exposed in Appendix C.

3. Kinetic and compartmental description

In this section, we will show that the discretized traffic flow model (4) (on a finite road) is formally kinetic with appropriate assumptions on g, and it can be interpreted in a compartmental context.

3.1. Kinetic models

Here we characterize kinetic system models based on the notations used in Feinberg (2019), where more details can be found on this model class. We assume that a kinetic model contains M species denoted by $\mathcal{X}_1, \ldots, \mathcal{X}_M$, and the species vector is $\mathcal{X} = [\mathcal{X}_1 \ \ldots \ \mathcal{X}_M]^T$. The basic building blocks of kinetic systems are *elementary reaction steps* of the form

$$C_j \to C'_j, \ j = 1, \ldots, R \tag{9}$$

where for $j = 1, \ldots, R$, $C_j = y_j^T \mathcal{X}$ and $C'_j = {y'_j}^T \mathcal{X}$ are the *complexes* and $y_j, y'_j \in \mathbb{N}_0^M$ are integer coefficients. The transformation shown in (9) means that during an elementary reaction step between the *reactant complex* C_j and *product complex* C'_j, $[y_j]_i$ items (molecules) of species $\mathcal{X}_i$ are consumed, and $[y'_j]_i$ items of $\mathcal{X}_i$ are produced for $i = 1, \ldots, M$. The reaction (9) is an *input* (resp. *output*) *reaction of species* $\mathcal{X}_i$ if $[y'_j]_i > 0$ (resp. $[y_j]_i > 0$).

Let $\chi(t) \in \overline{\mathbb{R}}_+^M$ denote the state vector corresponding to $\mathcal{X}$ for any $t \geq 0$ (in a chemical context, χ is the vector of concentrations of the species in $\mathcal{X}$). Then the ODEs describing the evolution of χ in the kinetic system containing the reactions (9) are given by

$$\dot{\chi} = \sum_{i=1}^{R} \mathcal{K}_i(\chi, t)[y'_i - y_i], \ \chi(0) \in \overline{\mathbb{R}}_+^M \tag{10}$$

where $\mathcal{K}_i : \overline{\mathbb{R}}_+^M \times \mathbb{R} \longrightarrow \mathbb{R}_+$ is the *rate function* corresponding to reaction step i, and determines the velocity of the transformation. For the rate functions, we assume the following for $i = 1, \ldots, R$:

(A4) $\mathcal{K}_i(\cdot, t)$ is locally Lipschitz continuous, and $\mathcal{K}_i(\chi, \cdot)$ is piecewise locally Lipschitz continuous with a finite number of discontinuities,

(A5) for $j = 1, \ldots, m$, $\mathcal{K}_i(\cdot, t)$ depends on χ_j if and only if $y_j > 0$,

(A6) $\mathcal{K}_i \geq 0$, and for $j = 1, \ldots, m$, $\mathcal{K}_i(\chi, t) = 0$ whenever $\chi_j = 0$ and $y_j > 0$,

(A7) There exist continuous nonnegative and strictly monotone (w.r.t. a partial order on $\overline{\mathbb{R}}_+^M$) functions $\underline{\mathcal{K}}_i, \overline{\mathcal{K}}_i : \overline{\mathbb{R}}_+^M \longrightarrow \mathbb{R}_{\geq 0}$ such that $\underline{\mathcal{K}}_i(\chi) \leq \mathcal{K}_i(\chi, t) \leq \overline{\mathcal{K}}_i(\chi)$ for all $t \geq 0$

These properties ensure the local existence and uniqueness of the solutions as well as the invariance of the nonnegative orthant for the dynamics in (10). From now on, a reaction from complex C_i to complex C'_i with rate function $\mathcal{K}_i$ will be denoted as $C_i \xrightarrow{\mathcal{K}_i} C'_i$. We will also suppress the t argument in the rate function if it does not explicitly depend on time.

A set of nonlinear ODEs given as $\dot{\chi} = f(\chi)$ is called *kinetic* if it can be written in the form (10) with appropriate rate functions $\mathcal{K}_i$. We remark that the representation (10) of a kinetic ODE is generally non-unique even if the rate functions are a priori fixed (Ács et al., 2016).

3.2. Kinetic representation of the traffic flow model

Using the above notions, we can give a kinetic interpretation for the TRM, where the species and the reaction steps have a clear physical meaning. For this purpose, we consider the TRM (4) on a finite road (with P cells).

Let us model each road cell $i \in I = \{1, \ldots, P\}$ as a compartment containing two homogeneously distributed species: units of occupied space N_i and units of free space S_i. The flow of vehicles between the consecutive cells (compartments) $i - 1$ and i (for $i \in \{2, \ldots, P\}$) is then represented by chemical reactions converting occupied space in one cell into occupied space on the next one, as follows

$$N_{i-1} + S_i \xrightarrow{\mathcal{K}_{i-1,i}} N_i + S_{i-1}, \quad i \in \{2, \ldots, P\}, \tag{11}$$

where $\mathcal{K}_{1-1,i}$ is the corresponding reaction rate. This model is represented in Fig. 2. Note that, in this representation, units of space can flow from cell $i - 1$ to cell i provided that a unit of occupied space is present in cell $i - 1$ and that a unit of free space is present in cell i. By recalling condition (A6) in Section 3.1, it is easy to see that the model in Eq. (11) naturally enforces that there can be no flow from cell $i - 1$ to cell i if cell $i - 1$ is empty (i.e. there is no unit of occupied space N_{i-1}) or if cell i is full (i.e. there is no unit of free space S_i).

Regarding the on and off-ramps in a given cell $i \in I$, they are respectively described by the following reaction steps

$$S_i \xrightarrow{\mathcal{K}_{\text{on},i}} N_i, \quad N_i \xrightarrow{\mathcal{K}_{\text{off},i}} S_i \tag{12}$$

where $\mathcal{K}_{\text{on},i}$ and $\mathcal{K}_{\text{off},i}$ are the reaction rates. These transformations express that during an elementary step of on-ramp (resp. off-ramp) reaction, a unit of free space (resp. occupied space) is consumed, and turned into a unit of occupied space. As for the boundary compartments $j \in \{1, P\}$, they are characterized by similar reaction steps, namely
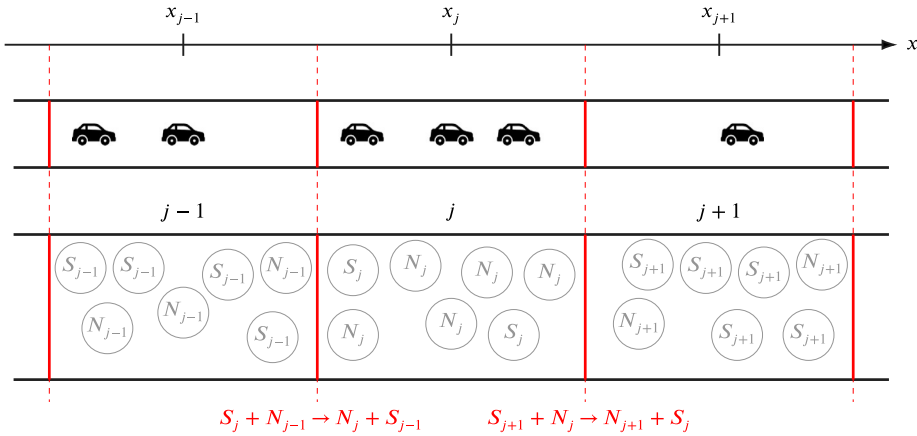
$$S_1 \xrightarrow{\mathcal{K}_{\text{in}}} N_1, \quad N_P \xrightarrow{\mathcal{K}_{\text{out}}} S_P \tag{13}$$

Fig. 2. Representation of the traffic reaction model interpretation of traffic flow. The discretized road (Top row) is seen as a sequence of compartments (Bottom row) containing "molecules" of free space S and occupied space N (represented as circles). The flow of vehicles along the road is then modeled by chemical reactions between the compartments (written in red).

where the reaction rates $\mathcal{K}_{\text{in}}$ and $\mathcal{K}_{\text{out}}$ are set to reflect the boundary conditions.

Let $n = (n_i : i \in I)$ and $s = (s_i : i \in I)$ denote the concentrations of occupied and free space in the compartment $i \in I$. Within our analogy, these quantities can respectively be seen as the equivalent of the density of vehicles and the density of free space in the cell. Then the kinetic differential system (10) corresponding to the kinetic model with reaction steps (11)–(12) is the system of ODEs defined by

$$\dot{n}_i = \mathcal{K}_{i-1,i}(n_{i-1}, s_i) - \mathcal{K}_{i,i+1}(n_i, s_{i+1}) + \mathcal{K}_{\text{on},i}(s_i, t) - \mathcal{K}_{\text{off},i}(n_i, t), \quad i \in I, \tag{14}$$

$$\dot{s}_i = \mathcal{K}_{i,i+1}(n_i, s_{i+1}) - \mathcal{K}_{i-1,i}(n_{i-1}, s_i) + \mathcal{K}_{\text{off},i}(n_i, t) - \mathcal{K}_{\text{on},i}(s_i, t), \quad i \in I, \tag{15}$$

where we adopt the notation $\mathcal{K}_{0,1}(n_0, n_1) \equiv \mathcal{K}_{\text{in}}(n, t)$ and $\mathcal{K}_{P,P+1}(n_P, n_{P+1}) \equiv \mathcal{K}_{\text{off}}(n, t)$.

Note that $\dot{n}_i + \dot{s}_i = 0$. Hence, $c_i = n_i + s_i$ is a first integral (conserved quantity) of the dynamics which can be interpreted as the maximal vehicle density in cell i. It is also clear that the conservation of c_i guarantees the boundedness of the solutions of (14)–(15). Substituting then $s_i = c_i - n_i$ into (14) (and assuming that $0 \leq n_i(0) \leq c_i$) gives (for $i \in I$)

$$\dot{n}_i = \mathcal{K}_{i-1,i}(n_{i-1}, c_i - n_i) - \mathcal{K}_{i,i+1}(n_i, c_{i+1} - n_{i+1}) + \mathcal{K}_{\text{on},i}(c_i - n_i, t) - \mathcal{K}_{\text{off},i}(n_i, t)$$

This last equation is equivalent to the TRM equation (4) when taking $n_i = \rho_i$ to be the vehicle density of the ith cell, $c_i = \rho_{\max}$ to be the maximal cell capacity, and defining the reaction rates as

$$\mathcal{K}_{i,i+1}(\rho, v) = g(\rho, v)/\Delta x, \quad i \in \{0, \dots, P\}, \tag{16}$$

and for $i \in I$, $\mathcal{K}_{\text{on},i}(\rho, t) = R_i(\rho, t)/\Delta x$, and $\mathcal{K}_{\text{off},i}(\rho, t) = S_i(\rho, t)/\Delta x$. A notable case is when we consider TRM with the decomposition $g = g_{\text{MAK}}$ introduced in Example 2. Then, the resulting reaction rates are exactly those obtained when considering the kinetic system under the so-called mass action kinetics (Chellaboina et al., 2009) assumption.

More generally, the kinetic interpretation of the TRM provides a new insight into the definition of fundamental diagrams, as modeled by the function $\rho \mapsto f(\rho)$ linking the flux to the density of vehicles. Indeed, the decomposition g used to define f, which involves both the density of vehicles ρ and its dual the free space density v, has a clear physical and kinetic interpretation: it models how free space is turned into occupied space by the flow of vehicles. It is clearly visible from Eq. (16) that there is a simple proportional relationship between the kinetic reaction rates and the speed-density relationship of the fundamental diagrams. This gives a transparent and physically meaningful mapping between traffic flows and kinetic models. Therefore, two main conclusions can be drawn. First, the TRM offers a complementary microscopic point-of-view on traffic where the particles being modeled are not vehicles but units of free and occupied space, and which has a clear and straightforward link to the quantities modeled by the macroscopic traffic model. Second, the TRM allows to propose and to interpret fundamental diagram relations based on a microscopic model for the transformations of free space and occupied space.

3.3. Application: Dynamical analysis of the ring topology

We conclude thus section with an example of how the kinetic interpretation of the TRM can be leveraged to deduce some properties of the model using kinetic system theory. In particular, we consider the special case when the TRM with P compartments has a ring topology (i.e. periodic boundary conditions) without on and off-ramps, and study the persistence of the dynamics and then the stability of the equilibria.

3.3.1. Persistence of the dynamics using kinetic theory

Following the kinetic interpretation made in Section 3, the TRM can be analyzed using the theory of kinetic systems. Indeed, the TRM is equivalent to the kinetic system defined by the reactions (11) and (13). Note in particular that the boundary reactions (13) can be merged into a single reaction linking the first and last cells, and given by

$$N_P + S_1 \xrightarrow{\mathcal{K}_{P,1}} N_1 + S_P.$$
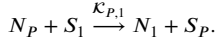
Since the reaction rates $\mathcal{K}_{i,i+1}$ are given by (16) and do not depend explicitly on time, and assuming that they are real analytic functions, we can use the results of Angeli et al. (2007) on the persistence of kinetic systems.

A nonnegative kinetic system is called *persistent* if no trajectory that starts in the interior of the orthant $\mathbb{R}_+^P$ has an ω-limit point on the boundary of $\mathbb{R}_+^P$. A non-empty set of species $\Sigma \subset \mathcal{X}$ is called a *siphon* if each input reaction associated to Σ is also an output reaction associated to Σ. A siphon is *minimal* if it does not contain (strictly) any other siphons. Naturally, the union of siphons is a siphon. The sufficient conditions for the persistence of the dynamics are the following Angeli et al. (2007): (1) there exists a positive linear conserved quantity (i.e., a first integral) for the dynamics, and (2) each siphon contains a subset of species, the state variables of which define a nonnegative linear first integral for the dynamics.

It is straightforward to see that Condition (1) is fulfilled, since $I_0 = \sum_{i=1}^{P} s_i + n_i$ is a conserved quantity for the system. For Condition (2), it can be checked that the only minimal siphons in the ring topology are: $\Sigma_N = \{N_1, \dots, N_P\}$, $\Sigma_S = \{S_1, \dots, S_P\}$, and $\Sigma_i = \{N_i, S_i\}$ for $i = 1, \dots, P$. Since $I_N = \sum_{i=1}^{P} n_i$, $I_S = \sum_{i=1}^{P} s_i$, and $I_i = n_i + s_i$ for $i = 1, \dots, P$ are also linear first integrals containing the state variables of Σ_N, Σ_S, and Σ_i respectively, Condition (2) is fulfilled. Therefore, the dynamics of the ring topology are persistent for any numerical flux F for which the corresponding reaction rates $\mathcal{K}_{i,i+1}$ satisfy the mild conditions described above. Note that in order to prove the persistence of the dynamics for a wide class of flux functions just by exploiting the ring structure, we needed both sets of state variables representing the density of vehicles as well as the density of free space.

3.3.2. Structure of equilibrium and stability

We first analyze the possible equilibrium points of the system. The proof of the next result can be found in Appendix B.2.

Proposition 3.1. *For the system of ODEs* (4) *resulting from the mass action kinetic TRM with a ring topology, the only possible equilibrium point* $(\rho_1^*, \dots, \rho_P^*)$ *is the one satisfying for any* $k \in I$

$$\rho_k^* = \bar{\rho} = \frac{1}{P} \sum_{i=1}^{P} \rho_i(0)$$

Hence, as one could have expected, the only possible equilibrium point for the system is the one where the vehicles distribute themselves uniformly across the (circular) road. Clearly there exist infinitely many equilibria for the system, but there is one unique positive equilibrium within each equivalence class $\mathcal{H}_c = \{\rho \in \Omega \mid \sum_{i=1}^{P} \rho_i = c\}$ defined by the conservation of vehicles. The next result elaborates on the stability of this equilibrium.

Proposition 3.2. *The equilibrium* $\bar{\rho}$ *is stable on* Ω.

Proof. We use the entropy-like Lyapunov function candidate well-known from the theory of reaction networks (Feinberg, 1987):

$$V(\rho) = \sum_{i=1}^{P} \left(\rho_i \left[\log \left(\frac{\rho_i}{\bar{\rho}} \right) - 1 \right] + \bar{\rho} \right). \tag{17}$$

Then,

$$\dot{V} = \frac{\omega}{\Delta x} \sum_{i=1}^{P} \log \left(\frac{\rho_i}{\bar{\rho}} \right) \left[\rho_{i-1}(\rho_{\max} - \rho_i) - \rho_i(\rho_{\max} - \rho_{i+1}) \right],$$

which gives

$$\dot{V} = \frac{\omega\bar{\rho}}{\Delta x} \sum_{i=1}^{P-1} \frac{\rho_i(\rho_{\max} - \rho_{i+1})}{\bar{\rho}} \left[\log \left(\frac{\rho_{i+1}}{\bar{\rho}} \right) - \log \left(\frac{\rho_i}{\bar{\rho}} \right) \right] + \frac{\rho_P(\rho_{\max} - \rho_1)}{\bar{\rho}} \left[\log \left(\frac{\rho_1}{\bar{\rho}} \right) - \log \left(\frac{\rho_P}{\bar{\rho}} \right) \right],$$

then we use the inequality $e^a(b - a) \leq e^b - e^a$ to give an upper bound such that

$$\frac{\Delta x}{\omega} \dot{V} \leq \sum_{i=1}^{P-1} (\rho_{\max} - \rho_{i+1})(\rho_{i+1} - \rho_i) + (\rho_{\max} - \rho_1)(\rho_1 - \rho_P)$$

$$= \sum_{i=1}^{P-1} \rho_{i+1}\rho_i - \rho_{i+1}^2 + \rho_1\rho_P - \rho_1^2 = \sum_{i=1}^{P} -\frac{1}{2}(\rho_i^2 - 2\rho_{i+1}\rho_i + \rho_{i+1}^2) = \sum_{i=1}^{P} -\frac{1}{2}(\rho_i - \rho_{i+1})^2 \leq 0.$$

Note that the entropy-like Lyapunov function V does not depend on the model parameters, and $\dot{V} < 0$ outside the equilibria. We also remark that the theory of kinetic and compartmental systems can still be used when the spatial discretization is non-uniform along the ring. In such a case, the analytical computation of the equilibrium is not straightforward. However, we know that the dynamics is persistent, and for any $c > 0$, there exists a unique strictly positive equilibrium in $\mathcal{H}_c$ which is stable with the Lyapunov function defined in Eq. (17), and asymptotically stable within $\mathcal{H}_c$. $\square$

It is important to add that the special case studied here can be greatly generalized using recent results. Persistence and stability can be similarly proved not only for the MAK decomposition used here, but for very general reaction rates and thus for a really wide set of fundamental diagrams for arbitrary strongly connected networks (Szederkényi et al., 2022). Moreover, we can handle explicitly time-varying transition rates (possibly resulting from changing conditions and/or external control) and determine a whole family of logarithmic Lyapunov functions in that case (Vághy and Szederkényi, 2023).

4. Analysis of TRM: Comparison with the CTM

In this section, we formally show that the TRM is equivalent to the Cell Transmission Model (CTM) (Daganzo, 1994) under some specific parametrization of the input capacity (i.e. cell supply function). Further analysis of the TRM is proposed in the Supplementary materials of this paper, where we show how the TRM can be interpreted as a REA algorithm and we analyze how it approximates shock waves (modified equations analysis).

In the CTM, the road is discretized into homogeneous cells of size Δx (indexed in the ascending order in the direction of circulation of the road). The number of vehicles inside a cell i is represented by a time-dependent function η_i. Consider some time step Δt. The evolution of the number of vehicles η_i from a time t to a time $t + \Delta t$ is described by the recurrence relation

$$\eta_i(t + \Delta t) = \eta_i(t) + y_i(t) - y_{i+1}(t),\tag{18}$$

where the quantity $y_i(t)$ represents the number of vehicles entering the cell i (from the cell $i - 1$) between t and $t + \Delta t$. These flows of vehicles are then assumed to be given, for any time t, by the relation

$$y_i(t) = \min\{\eta_{i-1}(t), Q_i(t), N_i(t) - \eta_i(t)\},\tag{19}$$

where $N_i(t)$ denotes the maximal number of vehicles the cell i can hold at time t, and $Q_i(t)$ is the so-called input capacity of the cell i, which describes the maximal number of vehicles that could flow into the cell. Note in particular that for any i and any t, $\eta_i(t) \in [0, N_i(t)]$.

Consider now the case where the maximal number of vehicles a cell can contain is constant, i.e. there exists some constant N such that for any i and any t, $N_i(t) = N$. Let us then take the input capacities Q_i defined by

$$Q_i(t) = \Delta t\, g\Big(\frac{\eta_{i-1}(t)}{\Delta x}, \frac{N - \eta_i(t)}{\Delta x}\Big).\tag{20}$$

Then, assuming that the CFL condition (8) is satisfied, we have $y_i(t) = Q_i(t)$ for any i and any t. Indeed, using the properties of g, we have on the one hand,

$$Q_i(t) = \Delta t\Big(g\Big(\frac{\eta_{i-1}(t)}{\Delta x}, \frac{N - \eta_i(t)}{\Delta x}\Big) - g\Big(0, \frac{N - \eta_i(t)}{\Delta x}\Big)\Big) \le \Delta t K_1\Big|\frac{\eta_{i-1}(t)}{\Delta x} - 0\Big| = K_1\frac{\Delta t}{\Delta x}\eta_{i-1}(t),$$

and similarly on the other hand,

$$Q_i(t) = \Delta t\Big(g\Big(\frac{N}{\Delta x}, \frac{N}{\Delta x}\Big) - g\Big(\frac{N}{\Delta x}, 0\Big)\Big) \le K_2\frac{\Delta t}{\Delta x}\big(N - \eta_i(t)\big).$$

Using then the fact that the CFL condition (8) implies that $K_1\Delta t/\Delta x \le 1$ and $K_2\Delta t/\Delta x \le 1$, we retrieve that $y_i(t) = Q_i(t)$.

Note then that the density of vehicles $\rho_i(t)$ inside the ith cell is obtained by dividing the number of vehicles $\eta_i(t)$ by the cell size Δx. Similarly, the maximal density of vehicles is $\rho_{\max} = N/\Delta x$. Hence, by dividing (18) by Δx, we obtain the relation:

$$\rho_i(t + \Delta t) = \rho_i(t) + \frac{y_i(t)}{\Delta x} - \frac{y_{i+1}(t)}{\Delta x}\tag{21}$$

where for any i,

$$\frac{y_i(t)}{\Delta x} = \frac{Q_i(t)}{\Delta x} = \frac{\Delta t}{\Delta x}\, g\big(\rho_{i-1}(t), \rho_{\max} - \rho_i(t)\big),$$

Hence, (21) coincide exactly with the recurrence relation defining the TRM (7). We then conclude that the CTM, when defined with the input capacities (20), fits into the TRM framework proposed in this work. This particular choice of input capacities simplifies greatly the expression (19) defining the flow of vehicles: the minimum disappears and we are left with the numerical fluxes of the TRM. In conclusion, the TRM elegantly incorporates in a compact (analytic) form the restrictions on the flux of vehicles allowed to travel from cell to the other. The resulting smoothness opens the door for the application of results on polynomial systems of ODEs for the analysis of the numerical properties of the TRM.

5. Possible extensions of the TRM

In this section we present two straightforward extensions of the TRM that allow to model traffic in more complex situations that those covered by the LWR model (1) on a unidirectional road.

5.1. Accounting for changing driving conditions

The TRM can be adapted to model roads with non-homogeneous driving conditions, may they be due to changes in the maximal vehicle density admissible along the road (due for instance to varying number of lanes) or more generally to external factors affecting the optimal flow of vehicles. Indeed, consider once again a road discretized into cells $i \in I$, and let $\rho_{\max}^{(i)}$ denote the capacity of the ith cell. We call *Extended TRM* the system of ODEs defined by

$$\dot{\rho}_i(t) = \frac{1}{\Delta x} \left(C_i(t) F_i(\rho_{i-1}, \rho_i) - C_{i+1}(t) F_{i+1}(\rho_i, \rho_{i+1}) + R_i(\rho_i, t) - S_i(\rho_i, t) \right), \quad i \in I, \quad t \geq 0$$

where for each $i \in I$, the numerical flux F_i is given by

$$F_i(u, v) = g(u, \rho_{\max}^{(i)} - v),$$

the function g is defined in the same way as in Section 2, and the function $t \mapsto C_i(t)$ takes values in $(0, 1]$ can be seen as local capacity drop factor which scales down the "ideal" flow of vehicles $F_i(\rho_{i-1}, \rho_i)$ between cells $i - 1$ and i, i.e. the flow of vehicles one should expect between these cells given their density states. By identification with the usual TRM, this factor can essentially be seen as a time-varying normalized free flow speed $v_{\max}$ at the interface between cells $i - 1$ and i, or within the kinetic compartmental interpretation, as a time-varying normalized reaction rate coefficient between compartments $i - 1$ and i. On the other hand, allowing the maximal capacity $\rho_{\max}^{(i)}$ to change across compartments allows for instance to account for changes in the number of lanes or for non-uniform discretizations of the road.

Following the same arguments as the ones used in Theorem 2.2, it is clear that the Extended TRM will yield solutions that preserve non-negativity and capacity. Besides, the extended TRM has been shown to accurately describe real-world traffic datasets in applications related to traffic state estimation (Pereira et al., 2022a) and short-term prediction (Pereira et al., 2022b). This is manly due to the local capacity drop factors C_i which allow to locally change the conditions at which traffic flows on the roads, hence allowing the TRM (which inherits from the seemingly simplistic LWR model) to recreate complex traffic patterns observed in the data.

To illustrate this last property of the Extended TRM, we present in Fig. 3 the results of a simulation study where traffic along a unidirectional road with a traffic light is modeled. To do so, we start by discretizing the road into compartments and consider that at the position $x = 0$ where the traffic light is located, the corresponding capacity drop coefficient $C(t)$ oscillates between two values: 1 when the traffic light is green, and 0 when it is red (cf. Figs. 3(a) and 3(b)). Following the kinetic interpretation of the TRM, this choice will effectively stop the flow of vehicles at $x = 0$ when the traffic light is red. The mass action kinetic decomposition is chosen, which in particular yields a polynomial system of ODEs which can be solved at arbitrary time steps with high accuracy using standard libraries.

The Extended TRM is run on a road of 5 km discretized into compartments of 5 m. The free flow speed of vehicles is set to 30 km/h and the simulation is run on a time horizon of 10 min, with light switches happening approximately every 2 min. The results presented in Figs. 3(c)–3(e) seem to show that the model manages to recreate both the wave propagations and the oscillatory nature the density variations due to the traffic light changes.
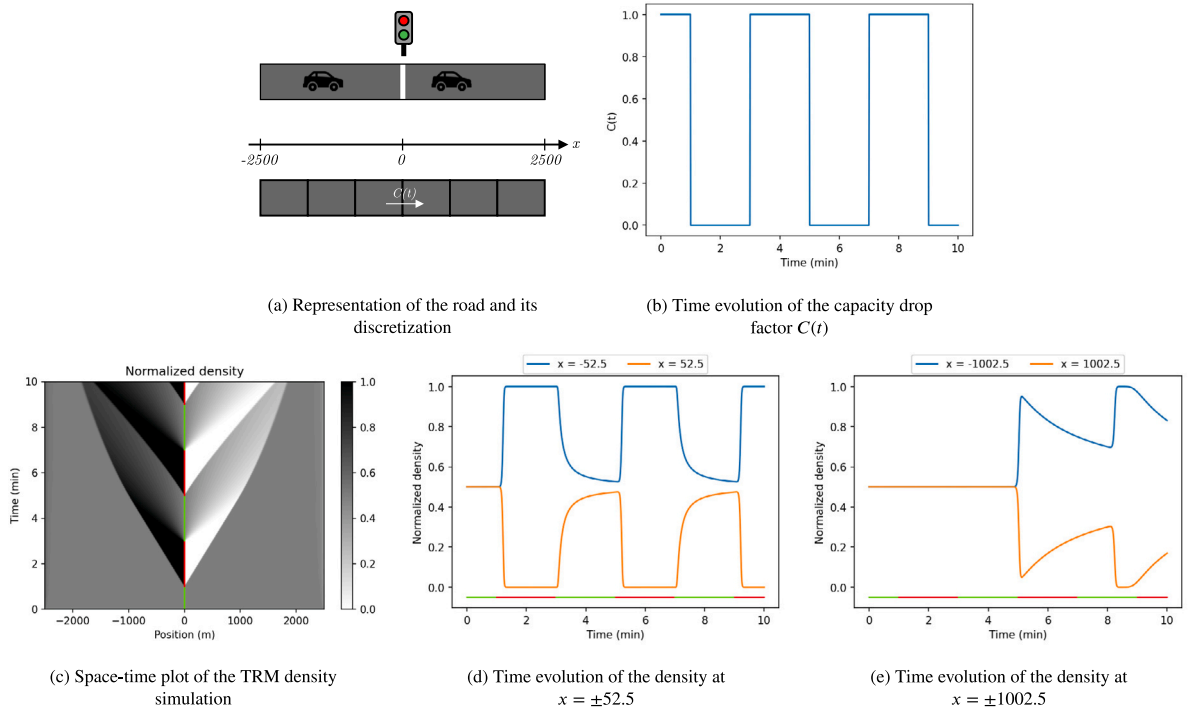
5.2. Accounting for road networks

The TRM can also be directly adapted to model traffic on networks. Indeed, following the kinetic and compartmental interpretation given in Section 3, traffic on a network can be assimilated to a compartmental chemical reaction network for which each compartment is now allowed to have more than two other neighboring compartments. Starting from a road network, modeled as a directed graph, each directed edge is discretized into compartments, and each intersection is replaced by an additional compartment. An example of such discretization is given in Fig. 4, and show in particular how the TRM can be extended to handle complex intersections. The *Network TRM* then takes the form of a system of ODEs defined as

$$\dot{\rho}_i(t) = \frac{1}{\Delta x} \left(\sum_{j \in \mathcal{N}_{\text{in}}(i)} F(\rho_j, \rho_i) - \sum_{k \in \mathcal{N}_{\text{out}}(i)} F(\rho_i, \rho_k) + R_i(\rho_i, t) - S_i(\rho_i, t) \right), \quad i \in I, \quad t \geq 0 \tag{22}$$

where for each compartment $i \in I$, $\mathcal{N}_{\text{in}}(i)$ denotes the set of compartments j that point to i (i.e. such that vehicles can move from j to i) and $\mathcal{N}_{\text{out}}(i)$ denotes the set of compartments k that i points to (i.e. such that vehicles can move from i to k).

Once again, following the same arguments as the ones used in Theorem 2.2, it is clear that the *Network TRM* will also yield solutions that preserve non-negativity and capacity. This qualifies the Network TRM to act as a generic link and node model for traffic networks according to the classification of Tampère et al. (2011). Following the categories in Tampère et al. (2011), the *Network TRM* extension is an unsignalized node model where supply and capacity constraints are handled in a balanced and continuous way. This latter property roots in fact in the balanced interaction of chemical species changing the concentrations in the compartments. In terms of supply constraint interaction rules (Tampère et al., 2011), the *Network TRM* generates them *implicitly*: free space concentrations are transformed into occupied ones dynamically, smoothly. In terms of the solution algorithm, the set of nonlinear ODEs guarantees the existence of a unique solution to the density propagation across all link and node compartments (via Lipschitz continuity Khalil, 2002). Node and link models are described in a unified way with TRM. Links and nodes rely on the reaction rate governed exchange of material (vehicle) in- and outflows. Merging and diverging is handled by in- and outgoing flows (see, Eq. (22)). Besides, the *Network TRM* can readily be further extended in order to account for varying road conditions using the same approach as the one outlined for the Extended TRM. In practice, the link between the TRM and chemical reaction networks can be leveraged to deduce persistence and Lyapunov stability results that generalize even to time-varying networks, the properties of which are outlined in Section 3.3 (Vághy and Szederkényi, 2022; Szederkényi et al., 2022; Szederkenyi and Vaghy, 2022).

(a) Representation of the road and its discretization

(b) Time evolution of the capacity drop factor $C(t)$

(c) Space-time plot of the TRM density simulation

(d) Time evolution of the density at $x = \pm 52.5$

(e) Time evolution of the density at $x = \pm 1002.5$

Fig. 3. Extended TRM simulation of the normalized density on a road with a traffic light. The red and green lines indicate when the capacity drop factor is set to 0 (red lines) or to 1 (green lines).
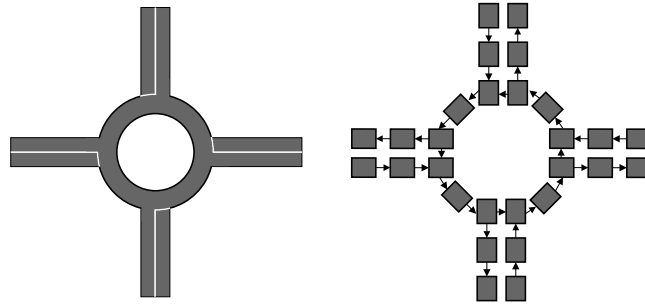
Fig. 4. TRM discretization *(Right)* of a roundabout *(Left)*.

6. Conclusions

Traffic Reaction Model (TRM), a family of Finite Volume Methods for segmenting certain hyperbolic Partial Differential Equations arising in traffic flow modeling, has been presented in the paper. First, the proposed numerical approximation scheme is consistent, monotone, nonnegative, capacitated, and conservative, even under non-zero sink and source terms. Second, the resulting system of nonlinear ODE models enables us to formally view traffic flow models as chemical reaction networks. In the kinetic model formulation, two dual state variables appear representing traffic density and the density of free space, respectively. These dual densities enable a proper factorization of the nonlinearity in the original PDE, as done by the function $g()$, and also allow us to define multiple meaningful numerical fluxes.

We have compared the TRM to other known popular discretization schemes, and clarified their relations. Here we emphasize that TRM is equivalent to the CTM for a particular choice of input capacities. Numerical results show that the convergence properties of the proposed model are comparable to other popular schemes. The main benefits of the proposed modeling approach are the possibility to represent the system model in the form of smooth ODEs which is often required to apply advanced nonlinear control techniques, and to use the tools of compartmental systems and reaction network theory in the dynamical analysis of traffic models. The latter one was illustrated through the example of the ring topology, where the robust persistence and stability of the dynamics were shown using a Petri net representation (containing also both sets of state variables), and a parameter-free logarithmic Lyapunov

function, respectively. Finally, we have presented the possible extensions of the model firstly in the form of a time-varying nonlinear system, with basically the same physical interpretation, to describe capacity changes due to e.g., traffic lights, and secondly, as a straightforward network formulation which can be used to model an arbitrary road (directed graph) structure, thus allowing to better model real traffic data (Pereira et al., 2022a,b).

Further work will be focused on structured stability analysis, state estimation, and robust control design. An interesting research direction can be to further analyze the dual variable triggered parametrization of $f(\rho)$ within the framework of variational theory in order to see how the Hamilton–Jacobi representation (see, Laval and Leclercq (2013)) is changed.

CRediT authorship contribution statement

M. Pereira: Data curation, Formal analysis, Investigation, Methodology, Project administration, Software, Validation, Visualization, Writing – original draft, Writing – review & editing, Resources. **B. Kulcsár:** Conceptualization, Formal analysis, Funding acquisition, Methodology, Supervision, Validation, Writing – original draft, Writing – review & editing. **Gy. Lipták:** Conceptualization, Data curation, Formal analysis, Investigation, Methodology, Resources, Software, Writing – original draft. **M. Kovács:** Funding acquisition, Supervision. **G. Szederkényi:** Conceptualization, Funding acquisition, Methodology, Supervision, Validation, Writing – original draft, Writing – review & editing.

Declaration of competing interest

The authors declare that they have no known competing financial interests or personal relationships that could have appeared to influence the work reported in this paper.

Financial disclosure

Appendix A. Well-posedness of the traffic flow PDE

Lemma A.1. *Let $T > 0$. Let $f : \mathbb{R} \to \mathbb{R}$ be bounded and locally Lipschitz-continuous, and let $\psi : [0, T] \times \mathbb{R} \times \mathbb{R} \to \mathbb{R}$ such that*

- *$[(t, x) \in [0, T] \times \mathbb{R} \mapsto \psi(t, x, u)]$ is bounded and Lipschitz-continuous, uniformly in $u \in \mathbb{R}$,*
- *$[u \in \mathbb{R} \mapsto \psi(t, x, u)]$ is bounded and locally Lipschitz-continuous, uniformly in $(t, x) \in [0, T] \times \mathbb{R}$,*
- *the estimate $|\psi(t, x, u)| \leq C(1 + |u|)$ holds when $|u|$ is sufficiently large, for some $C > 0$ independent of t, x, u.*

Finally, let $u_0 \in L^1(\mathbb{R})$ such that u_0 is bounded. Then, the Cauchy problem defined by

$$\begin{cases} u_t + f(u)_x = \psi(t, x, u), & (t, x) \in [0, T] \times \mathbb{R}, \\ u(0, x) = u_0(x), & x \in \mathbb{R}, \end{cases} \tag{23}$$

admits weak solutions, among which there is exactly one solution $u \in C([0, T]; L^1(\mathbb{R}))$ satisfying the so-called entropy inequalities: for any convex function $\eta \in C^2(\mathbb{R})$ and function q such that $\dot{q} = \dot{\eta}\dot{f}$,

$$\int_0^T \int_{\mathbb{R}} \left(\eta(u)\phi_t + q(u)\phi_x - \dot{\eta}(u)\psi(t, x, u)\phi \right) dx \, dt \geq 0 \tag{24}$$

for any $\phi \in C_c^1([0, T] \times \mathbb{R})$ such that $\phi \geq 0$. This particular solution is called entropy solution of the Cauchy problem Eq. (23). Moreover, the entropy solution u depends continuously on the initial condition u_0 and is bounded.

Proof. This result a direct application of Theorems 3.1 and 6.1 of Chen and Karlsen (2005) in the case where the diffusion coefficient of the quasilinear anisotropic degenerate parabolic equation is zero.

Note that since the entropy solution satisfies $u \in C([0, T]; L^1(\mathbb{R}))$, it implies that for all $t_0 > 0$, $\lim_{t \to t_0} \int_{\mathbb{R}} |u(t, r) - u(t_0, r)| \, dr = 0$, and $\lim_{t \to 0+} \int_{\mathbb{R}} |u(t, r) - u_0(r)| \, dr = 0$. Hence, the regularity in time (measured in the above L_1-norm sense) of the conserved quantity under nonzero sink and source terms is guaranteed.

Appendix B. Additional proofs

B.1. Proof of Theorem 2.2

Proof. The numerical flow F is consistent since by definition and following Eq. (2), we have $F(u, u) = g(u, \rho_{\max} - u) = f(u)$ for any $u \in \Omega$. It is monotone due to the continuity assumption on f, consistency and the non-decreasing properties of g.

The TRM preserves non-negativity, since, for any $i \in I$, the right-hand side of Eq. (4), evaluated on the boundary $\rho_i = 0$, is nonnegative. Indeed, following the definitions of $g, g_{\mathrm{on}}, g_{\mathrm{off}}$, if $\rho_i = 0$, then

$$\dot{\rho}_i = \frac{1}{\Delta x} \left[g(\rho_{i-1}, \rho_{\max}) + R_i(0, t) \right] \geq 0.$$

since for any $t \geq 0$, $R_i(\rho_{\max}, t) = S_i(0, t) = 0$. Similarly, the TRM preserves bounded capacity, because the right-hand side of Eq. (4), evaluated on the capacity bound $\rho_i = \rho_{\max}$, yields $\dot{\rho}_i \leq 0$.

Finally, the discretization scheme Eq. (4) is conservative, because for any $n_l, n_r \in I$ such that $n_l < n_r$, the following is true:

$$\Delta x \sum_{i=n_l}^{n_r} \dot{\rho}_i = F(\rho_{n_l-1}, \rho_{n_l}) - F(\rho_{n_r}, \rho_{n_r+1}) + \sum_{i=n_l}^{n_r} R_i(\rho_i, t) - S_i(\rho_i, t),$$

meaning that the variation of the number of vehicles on a section of the road (i.e. the left hand side of this equation) is equal to the difference between the number of vehicles entering the section (at the boundary or through on-ramps) and the number of vehicles leaving the section (at the boundary or through off-ramps).

B.2. Proof of Proposition 3.1

Proof.

Since $(\rho_1^*, \ldots, \rho_P^*)$ is an equilibrium point, it must satisfy

$$F(\rho_{i-1}^*, \rho_i^*) = F(\rho_i^*, \rho_{i+1}^*), \quad i \in \{1, \ldots, P\}$$

where we write in particular $\rho_0^* = \rho_P^*$ and $\rho_{P+1}^* = \rho_1^*$. This gives in turn,

$$\rho_P^*(\rho_{\max} - \rho_1^*) = \rho_1^*(\rho_{\max} - \rho_2^*) = \cdots = \rho_{P-1}^*(\rho_{\max} - \rho_P^*).$$

Without loss of generality, assume that $\rho_1^* = \max_{i \in I} \rho_i^*$. We can then write,

$$\rho_1^*(\rho_{\max} - \rho_2^*) - \rho_1^*(\rho_{\max} - \rho_1^*) = \rho_P^*(\rho_{\max} - \rho_1^*) - \rho_1^*(\rho_{\max} - \rho_1^*)$$

which gives

$$\rho_1^*(\rho_1^* - \rho_2^*) = (\rho_{\max} - \rho_1^*)(\rho_P^* - \rho_1^*)$$

and therefore

$$\underbrace{\rho_1^*}_{\geq 0} \underbrace{(\rho_1^* - \rho_2^*)}_{\geq 0} + \underbrace{(\rho_{\max} - \rho_1^*)}_{\geq 0} \underbrace{(\rho_1^* - \rho_P^*)}_{\geq 0} = 0$$

We have three cases.

- If $\rho_1^* = 0$, then since $\rho_1^* = \max_{i \in I} \rho_i^*$, we have $\rho_1^* = \rho_2^* = \cdots = \rho_P^* = 0$.
- If $\rho_1^* = \rho_{\max}$, then since $\rho_1^*(\rho_{\max} - \rho_2^*) = \rho_P^*(\rho_{\max} - \rho_1^*) = 0$, we have $\rho_2^* = \rho_{\max}$. And since $\rho_2^*(\rho_{\max} - \rho_3^*) = \rho_1^*(\rho_{\max} - \rho_2^*) = 0$, we have $\rho_3^* = \rho_{\max}$. By continuing this process, we then prove that $\rho_1^* = \rho_2^* = \cdots = \rho_P^* = \rho_{\max}$.
- If $\rho_1^* \neq 0$ and $\rho_1^* \neq \rho_{\max}$: then we must have $\rho_P^* = \rho_1^* = \rho_2^* = \max_{i \in I} \rho_i^*$. Hence we can apply the same result to prove that $\rho_1^* = \rho_2^* = \rho_3^* = \max_{i \in I} \rho_i^*$, and continue to do iteratively until we prove that $\rho_{P-2}^* = \rho_{P-1}^* = \rho_P^* = \max_{i \in I} \rho_i^*$. Hence we have $\rho_1^* = \rho_2^* = \cdots = \rho_P^*$.

In all three cases we proved that $\rho_1^* = \rho_2^* = \cdots = \rho_P^*$, which is clearly equal to $(1/P) \sum_{i \in I} \rho_i^*$.

Note then that the quantity

$$\bar{\rho}(t) = \frac{1}{P} \sum_{i=1}^{P} \rho_i(t)$$

satisfies

$$\dot{\bar{\rho}}(t) = (F(\rho_P, \rho_1) - F(\rho_P, \rho_1))/P = 0$$

since the TRM is conservative. Hence, $\bar{\rho}(t)$ is conserved through time, meaning that $\bar{\rho}(t) = (1/P) \sum_{i \in I} \rho_i^* = \bar{\rho}(0) = \bar{\rho}$. We can then conclude that $\rho_1^* = \rho_2^* = \cdots = \rho_P^* = \bar{\rho}$.
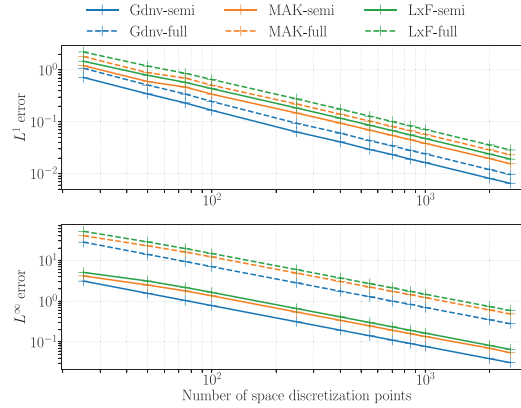
Fig. C.5. L^1-norm and L^∞-norm errors of the shock wave discretization for various numbers of segments P.

Appendix C. Empirical accuracy and convergence test for the trm

Consider a source and sink term free traffic flow model. The empirical accuracy tests are carried out with the parameters $\omega = 1$, $\rho_{\max} = 100$, and $\Delta x = L/P$, where $L = 20$ is the length of the examined segment, and N is the number of discrete segments. The end time is $T = 2/60$. We also consider that we have reflexive boundary conditions, i.e. we set $\rho_{-1} = \rho_0$ and $\rho_{P+1} = \rho_P$. We compare the performances of the semi-discrete scheme Eq. (4) and of the fully-discrete scheme Eq. (7) in terms of accuracy, for increasing numbers of space discretization points P. First, the system of ODEs of the semi-discrete scheme is solved numerically (Runge-Kutta approximation). Second, the time step of the fully discrete scheme is systematically set to $\Delta x/(2v_{\max})$ (following Theorem 2.4).

First, we introduce the time dependent error function e, which is the spatial L^1-norm error in each time t as follows

$$e(t) = \sum_{i=1}^{P} \int_{x_{i-1/2}}^{x_{i+1/2}} \left| \rho(x,t) - \rho_i(t) \right| dx, \tag{25}$$

where $\rho(x,t)$ denotes the value of the true solution of the PDE and $\rho_i(t)$ denotes, for the i-th cell, either the solution of the ODE system of the semi-discrete scheme or a piecewise constant reconstruction obtained from the quantities computed by the fully discrete scheme (and equal to ρ_i^n in each interval $[t_n, t_{n+1}]$). This spatial error term is computed analytically for each t and arbitrary values of $\rho_i(t)$, in the case of Riemann problems, using the closed forms for $\rho(x,t)$ provided by Leveque (1992). After that, we can define the L^1- and L^∞-norm of the spatial error function e as follows

$$\|e\|_1 = \int_0^T e(t)\,dt \quad \text{and} \quad \|e\|_\infty = \max_{0 \leq t \leq T} e(t).$$

C.1. Shock wave

Consider the Riemann-problem with the initial condition

$$\rho(x,0) = \begin{cases} 0.1\rho_{\max} & \text{if } x < L/2 \\ 0.8\rho_{\max} & \text{otherwise,} \end{cases}$$

which induces a solution consisting of a shock wave. Fig. C.5 shows the discretization errors of various monotone discretization schemes (both semi and fully discrete): the mass action kinetic (MAK) TRM Eq. (5), the Godunov (Gdnv) scheme Eq. (6), and the modified Lax-Friedrichs (LxF) scheme.[3] The errors decrease approximately as $\mathcal{O}(P^{-1})$ for all (semi and fully discrete) schemes, and the semi-discrete formulation of a given scheme systematically over-performs its fully discrete formulation. This is expected as the fully-discrete formulation add additional error due to the time discretization. If we compare the semi or fully discrete schemes with one another, the Godunov scheme systematically overperforms the other two, which display similar errors.

C.2. Rarefaction wave

Consider the Riemann-problem with the initial condition

$$\rho(x,0) = \begin{cases} 0.8\rho_{\max} & \text{if } x < L/2 \\ 0.1\rho_{\max} & \text{otherwise,} \end{cases}$$

---

[3] Numerical flux given by $F(u,v) = (f(u) + f(v))/2 + d(u-v)$ for $d \geq \omega\rho_{\max}/2$. Note that LxF is not a kinetic scheme.
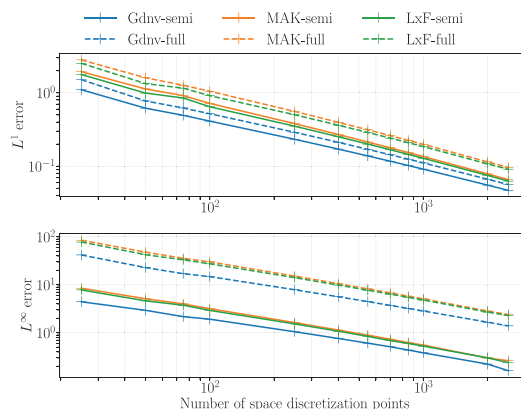
Fig. C.6. L^1-norm and L^∞-norm errors of the rarefaction wave discretization for various numbers of segments P.

which induces this time a solution consisting of a rarefaction wave. The discretization errors associated with this choice of initial condition are given in Fig. C.6. Once again, the semi-discrete formulations overperform compare to the fully-discrete ones, and the Godunov scheme overperforms compared to the other two schemes, that display similar errors. But this time, the errors at a slightly lower order of $\mathcal{O}(P^{-3/4})$. This difference could be explained by the fact that (spatially) piecewise constant reconstructions are used here to approximate a continuous rarefaction fan.

Appendix D. Supplementary data

Supplementary material related to this article can be found online at https://doi.org/10.1016/j.trc.2023.104435.

References

Ács, B., Szederkényi, G., Tuza, Z., Tuza, Z.A., 2016. Computing all possible graph structures describing linearly conjugate realizations of kinetic systems. Comput. Phys. Comm. 204, 11–20.

Angeli, D., De Leenheer, P., Sontag, E.D., 2007. A Petri net approach to the study of persistence in chemical reaction networks. Math. Biosci. 210 (2), 598–618.

Bressan, A., 2000. Hyperbolic Systems of Conservation Laws. The One Dimensional Cauchy Problem. Oxford University Press.

Chainais-Hillairet, C., Champier, S., 2001. Finite volume schemes for nonhomogeneous scalar conservation laws: error estimate. Numer. Math. 88 (4), 607–639.

Chaves, M., Sontag, E., 2002. State-estimators for chemical reaction networks of Feinberg–Horn–Jackson zero deficiency type. Eur. J. Control 8, 343–359.

Chellaboina, V., Bhat, S., Haddad, W., Bernstein, D., 2009. Modeling and analysis of mass-action kinetics – nonnegativity, realizability, reducibility, and semistability. IEEE Control Syst. Mag. 29, 60–78.

Chen, G., Karlsen, K., 2005. Quasilinear anisotropic degenerate parabolic equations with time-space dependent diffusion coefficients. Commun. Pure Appl. Anal. 4 (2).

Coogan, S., Arcak, M., 2015. A compartmental model for traffic networks and its dynamical behavior. IEEE Trans. Automat. Control 60 (10), 2698–2703.

Coogan, S., Arcak, M., 2016. Stability of traffic flow networks with a polytree topology. Automatica 66, 246–253.

Csikós, A., Charalambous, T., Farhadi, H., Kulcsár, B., Wymeersch, H., 2017. Network traffic flow optimization under performance constraints. Transp. Res. C 83, 120–133.

Csikos, A., Kulcsar, B., 2017. Variable speed limit design based on mode dependent cell transmission model. Transp. Res. C 85, 429–450.

Dabiri, A., Kulcsár, B., 2015. Freeway traffic incident reconstruction – A bi-parameter approach. Transp. Res. C 58, 585–597.

Dabiri, A., Kulcsár, B., Köröğlu, H., 2017. Distributed LPV state-feedback control under control input saturation. IEEE Trans. Automat. Control 62 (5), 2450–2456.

Daganzo, C., 1994. The cell transmission model: A dynamic representation of highway traffic consistent with the hydrodynamic theory. Transp. Res. B 28 (4), 269–287.

Daganzo, C., 2005. A variational formulation of kinematic waves: basic theory and complex boundary condition. Transp. Res. B 39, 187–196.

Érdi, P., Tóth, J., 1989. Mathematical Models of Chemical Reactions: Theory and Applications of Deterministic and Stochastic Models. Manchester University Press.

Eymard, R., Gallouet, T., Herbin, R., 2000. Finite Volume Methods (in: Handbook of Numerical Analysis). Elsevier.

Farina, L., Rinaldi, S., 2000. Positive Linear Systems: Theory and Applications, Vol. 50. John Wiley & Sons.

Feinberg, M., 1987. Chemical reaction network structure and the stability of complex isothermal reactors - I. The deficiency zero and deficiency one theorems. Chem. Eng. Sci. 42 (10), 2229–2268.

Feinberg, M., 2019. Foundations of Chemical Reaction Network Theory. Springer.

Garavello, M., Han, K., Piccoli, B., 2016. Models for Vehicular Traffic on Networks, Vol. 9. American Institute of Mathematical Sciences Springfield, MO, USA.

Godunov, S., 1959. A finite difference method for the numerical computation of discontinuous solutions of the equations of fluid dynamics. Mat. Sb. 47, 271–306.

Haddad, W.M., Chellaboina, V., Hui, Q., 2010. Nonnegative and Compartmental Dynamical Systems. Princeton University Press.

Haight, F., 1963. Mathematical Theories of Traffic Flow. Academic Press.

Jacquez, J.A., Simon, C.P., 1993. Qualitative theory of compartmental systems. SIAM Rev. 35 (1), 43–79.

Jin, W.-L., 2021. Introduction to Network Traffic Flow Theory: Principles, Concepts, Models, and Methods. Elsevier.

Karafyllis, I., Bekiaris-Liberis, N., Papageorgiou, M., 2018. Feedback control of nonlinear hyperbolic PDE systems inspired by traffic flow models. IEEE Trans. Automat. Control 64 (9), 3647–3662.

Karafyllis, I., Papageorgiou, M., 2019. Feedback control of scalar conservation laws with application to density control in freeways by means of variable speed limits. Automatica 105, 228–236.

Khalil, H.K., 2002. Nonlinear Systems. Prentice Hall.

Laval, J.A., Chilukuri, B.R., 2016. Symmetries in the kinematic wave model and a parameter-free representation of traffic flow. Transp. Res. B 89, 168–177.

Laval, J.A., Leclercq, L., 2013. The Hamilton–Jacobi partial differential equation and the three representations of traffic flow. Transp. Res. B 52, 17–30.

Leveque, R., 1992. Numerical Methods for Conservation Laws. Birkhauser.

LeVeque, R.J., et al., 2002. Finite Volume Methods for Hyperbolic Problems, Vol. 31. Cambridge University Press.

Lighthill, M., Whitham, G., 1955. On kinematic waves II.: A theory of traffic flow on long crowded roads. Proc. R. Soc. Lond. Ser. A Math. Phys. Eng. Sci. 229 (1178), 317–345.

Newell, G., 1993a. A simplified theory of kinematic waves in highway traffic, part I: General theory. Transp. Res. B 27B, 281–287.

Newell, G., 1993b. A simplified theory of kinematic waves in highway traffic, part II: Queing at freeway bottlenecks. Transp. Res. B 27B, 289–303.

Newell, G., 1993c. A simplified theory of kinematic waves in highway traffic, part III: Multi-destination flows. Transp. Res. B 27B, 305–313.

Papageorgiou, M., 1983. Applications of Automatic Control Concepts To Traffic Flow Modeling and Control. Springer-Verlag.

Pereira, M., Baykas, P.B., Kulcsár, B., Lang, A., 2022a. Parameter and density estimation from real-world traffic data: A kinetic compartmental approach. Transp. Res. B 155, 210–239.

Pereira, M., Lang, A., Kulcsár, B., 2022b. Short-term traffic prediction using physics-aware neural networks. Transp. Res. C 142, 103772.

Piccoli, B., Rascle, M. (Eds.), 2013. Modeling and Optimization of Flows on Network. In: Lecture notes in Mathematics, Springer.

Richards, P., 1956. Shock waves on the highway. Oper. Res. 4 (1), 42–51.

Samardzija, N., Greller, L.D., Wassermann, E., 1989. Nonlinear chemical kinetic schemes derived from mechanical and electrical dynamical systems. J. Chem. Phys. 90 (4), 2296–2304.

Shinar, G., Feinberg, M., 2010. Structural sources of robustness in biochemical reaction networks. Science 327, 1389–1391.

Siri, S., Pasquale, C., Sacone, S., Ferrara, A., 2021. Freeway traffic control: A survey. Automatica 130, 109655.

Sontag, E., 2001. Structure and stability of certain chemical networks and applications to the kinetic proofreading model of T-cell receptor signal transduction. IEEE Trans. Automat. Control 46, 1028–1047.

Szederkényi, G., Ács, B., Lipták, G., Vághy, M.A., 2022. Persistence and stability of a class of kinetic compartmental models. J. Math. Chem. 60 (6), 1001–1020.

Szederkényi, G., Magyar, A., Hangos, K., 2018. Analysis and Control of Polynomial Dynamic Models with Biological Applications. Academic Press.

Szederkenyi, G., Vaghy, M.A., 2022. Persistence and stability of generalized ribosome flow models with time-varying transition rates.

Tampère, C.M., Corthout, R., Cattrysse, D., Immers, L.H., 2011. A generic class of first order node models for dynamic macroscopic simulation of traffic flows. Transp. Res. B 45 (1), 289–309.

Tordeux, A., Costeseque, G., Herty, M., Seyfried, A., 2018. From traffic and pedestrian follow-the-leader models with reaction time to first order convection-diffusion flow models. SIAM J. Appl. Math. 78 (1), 63–79.

Treiber, M., Kesting, A., Thiemann, A., 2013. Traffic Flow Dynamics: Data, Models and Simulation. Springer.

Vághy, M.A., Szederkényi, G., 2022. Lyapunov stability of generalized ribosome flows. IFAC-PapersOnLine 55 (18), 56–61.

Vághy, M.A., Szederkényi, G., 2023. Persistence and stability of generalized ribosome flow models with time-varying transition rates. PLoS One 18 (7), e0288148.